

S1 Straightening of the membrane during washing

During cutting and punching, the membrane is likely to collapse and stick to the channel walls (figure S1a), while during washing, the device swells and the membrane straightens (figure S1b). During drying, the membrane shrinks the fastest because it is the thinnest structure.^{1,2} Therefore, it is under tension during the drying process, which prevents the membrane from collapsing back against the channel walls. After the drying step, the membrane is straight (figure S1c), otherwise the washing cycle can be repeated.

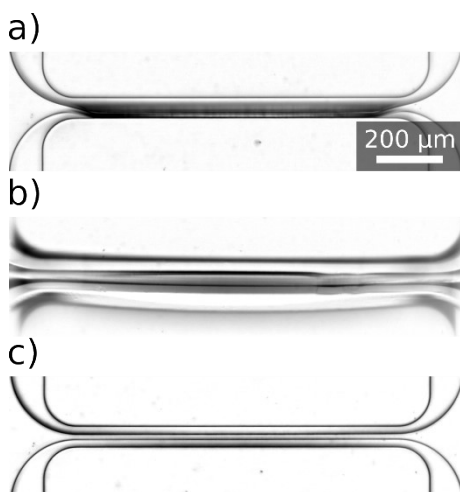


Figure S1: Device before binding. **a)** Collapsed membrane sticking to the channel walls. **b)** Swollen device during drying. The membrane is straightened. **c)** Device after drying with straight membrane.

S2 Evaluation of device binding

The aspect ratio of the membranes is at the upper manufacturing limit. In order to build devices with a reproducible functionality, it is mandatory to check the membrane for proper binding. The membrane is checked for complete binding by optical microscopy. If the membrane is not completely bonded to the glass slide, a three-phase contact line will form between the PDMS, air and the microscope slide (figure S2). If no contact lines are observed, one channel is filled with water and the pressure inside the channel is increased. This deflects the membrane and it is checked for leakage.

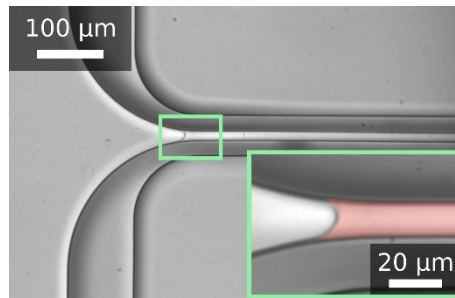


Figure S2: Improperly bonded membrane. The membrane forms a three-phase contact line with the glass slide and the air in the gap between the slide and the membrane. Insert: Zoom in on the three-phase contact line. The air gap between the membrane and the glass slide is highlighted in red.

S3 Determination of buckle positions

The wavelength of the deflection pattern is determined by measuring the position of the ‘nodes’, i.e., the point at which the deflection pattern passes through $z = 0$ at any y -position of a given x -position ($w(x,y) = 0, y \in [0,b]$), (figure S3a & b, top). The length of a buckle is the distance between two adjacent nodes (indicated by red dashed lines; figure S3a & b top) and defines $1/2\lambda$. The micrograph of the deflection pattern is a 2D representation of the 3D shape (deflection pattern). By averaging the pixel intensities in the z -direction, a 1D representation of the deflection pattern is obtained (figure S3a & b, bottom, blue line). Each node corresponds to a maximum in this intensity profile (figure S3a & b, red dashed line), which is fitted by a Gaussian fit (figure S3a & b, green line).

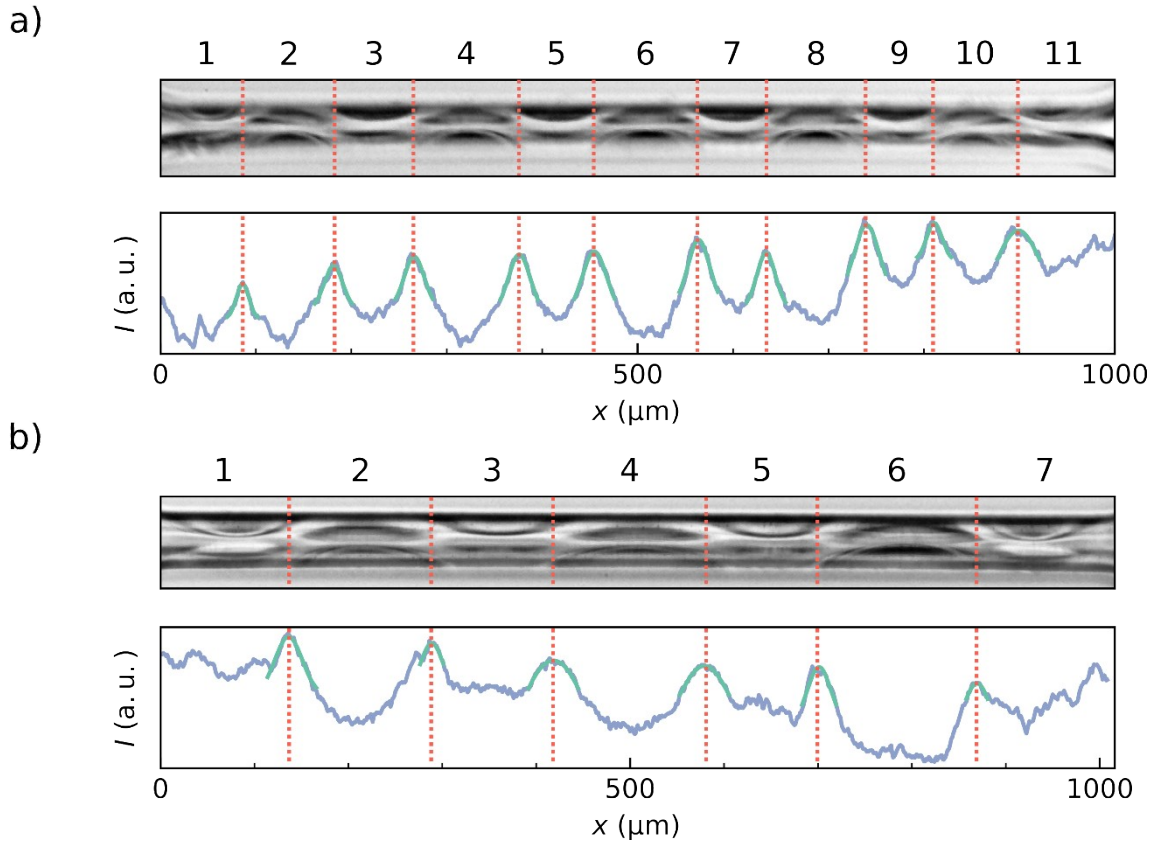


Figure S3: a) & b) Top: Micrograph of the deflection pattern of a PDMS membrane, with node positions highlighted by red lines. a) & b) Bottom: Intensity profile of the micrograph (1D projection) (blue line), with Gaussian fits of the node positions (green lines) and highlighted maxima of the fits corresponding to the node positions (red dashed line). a): $\phi_{iso} = 1.000$, b): $\phi_{iso} = 0.972$.

S4 Velocity field measurements

The velocities from which the flow rates Q^* were calculated are obtained by PIV. Tracking particles in the isopropanol-water mixture (figure S4a) gives the flow fields in the channels (figure S4b). Averaging the flow fields with the flow direction gives the flow profile perpendicular to the channel (figure S4c & d, left side). The flow profiles show a parabolic flow (figure S4c & d, left side, solid lines). The maximum velocity V_{max} depends linear on the pressure, since isopropanol-water mixtures show the behavior of Newtonian fluids (figure S4c & d, right side). The average velocity under the assumption of laminar flow is used to calculate Q^* .

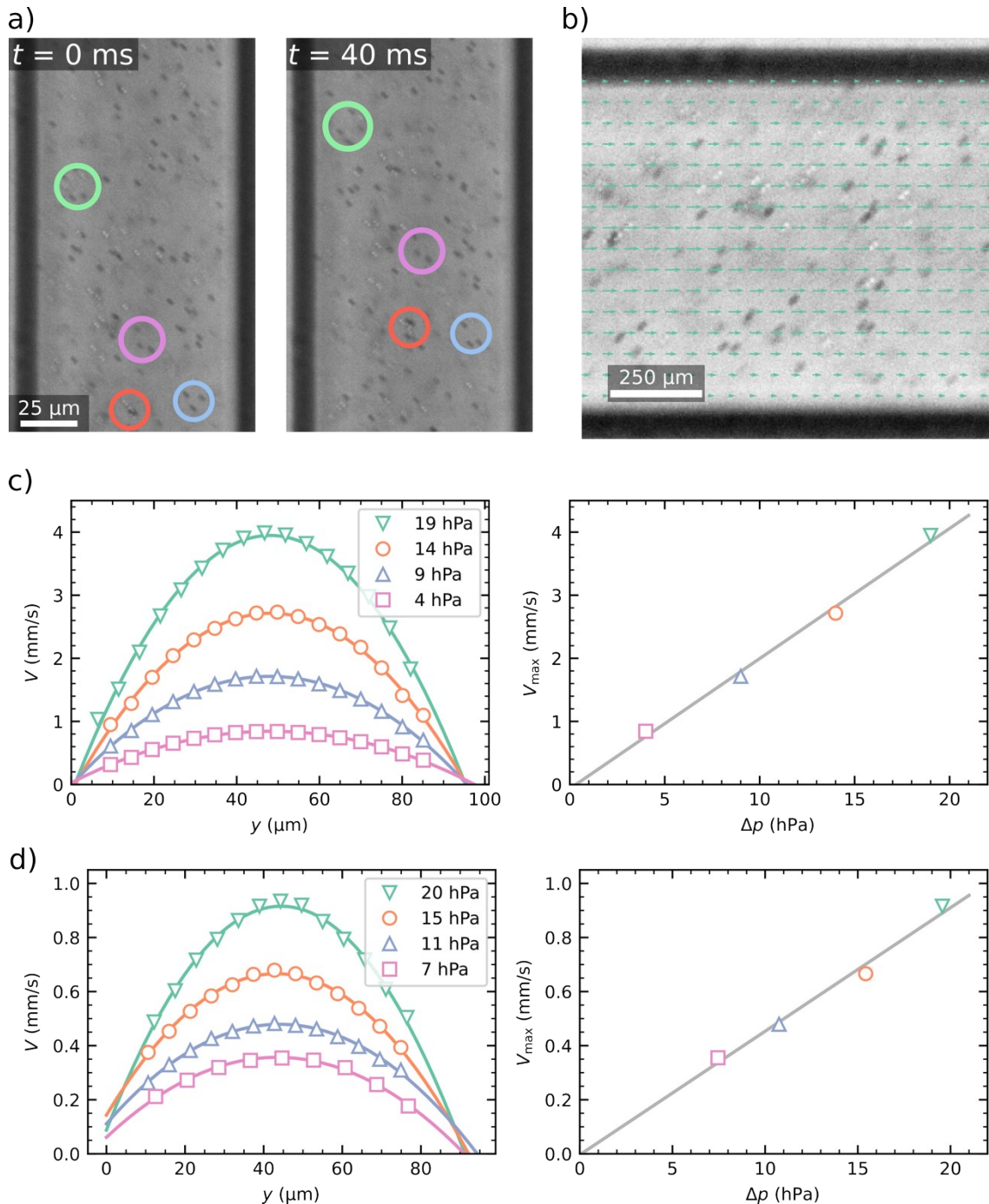


Figure S4: a) Single frames of a PIV measurement at $\phi_{iso} = 0.960$ and $\Delta p = 4 \text{ hPa}$. Exemplary, different particle formations in the solvent mixtures are highlighted at $t = 0 \text{ ms}$ and $t = 40 \text{ ms}$. b) Flow field of the solvent mixture of $\phi_{iso} = 0.960$ caused by

$\Delta p = 4 \text{ hPa}$. c) & d) left side: Average flow profiles in the microchannel, fitted with a parabolic flow profile. d) right side: Maximum velocity V_{max} from the flow profiles depending on the pressure p . c) $\phi_{iso} = 0.960$, d) $\phi_{iso} = 1.000$.

S5 Correction terms for the hydraulic resistance

As ϕ_{iso} increases, PDMS begins to swell, resulting in a slight reduction in channel cross-section. To consider only the changes caused by buckling of the membrane, $R(\phi_{iso})$ was corrected for the components caused by the change in cross-section due to pure swelling. This was done by introducing the factor f_{hc} , which rescales $R(\phi_{iso})$ to an initial channel cross-section at volume fractions of $\phi_{iso} = 0$. f_{hc} is the ratio of the geometric dependencies of $R(\phi_{iso})$ for rectangular channels at ϕ_{iso} and $\phi_{iso} = 0$. f_{hc} is defined as

$$f_{hc} = \frac{(1 - 0.63h_c/b)bh_c^3}{(1 - 0.63h_{c,\phi=0}/b)bh_{c,\phi=0}^3} \quad (S1),$$

where h_c is the channel height at ϕ_{iso} and $h_{c,\phi=0}$ is the initial channel height at $\phi_{iso} = 0$, and b is the width of the channels. b is assumed to be 200 μm , since no changes in b were detected. h_c was measured at the point where no buckling occurs in the micrographs used for PIV analysis. $R(\phi_{iso})/\eta$ compared to $R^*(\phi_{iso})/\eta$ are shown in Figure S5.

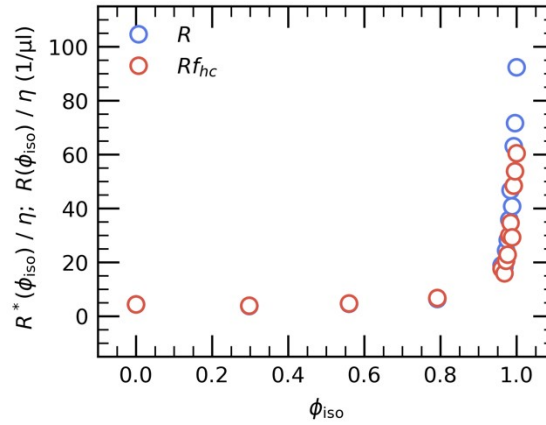


Figure S5: Hydraulic resistance $R(\phi_{iso})$, normalized by the viscosity, and hydraulic resistance corrected by f_{hc} , $R^*(\phi_{iso}) = R(\phi_{iso})f_{hc}$, normalized by the viscosity, versus ϕ_{iso} . The microfluidic channels with the membrane have the initial dimensions of $h_m = h_c = 20 \mu\text{m}$, $a = 1000 \mu\text{m}$, and $b = 200 \mu\text{m}$

S6 Swelling data

The swelling factor γ was determined by tracking the relative positions of the corners of micropillar arrays before and after swelling (figure S6 left & right). The relative positions of the corners to each other are described by the distances between the pillars $r_i - r_j$, from which γ is calculated by the ratio of the swollen and the un-swollen distances.

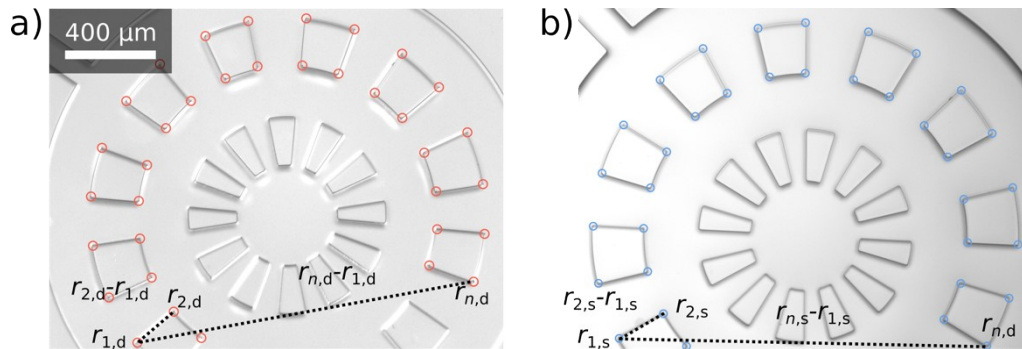


Figure S6: Swelling of the PDMS micropillars array. The relative positions of the micropillar edges shift during swelling. Left: PDMS pillar array at $\phi_{iso} = 0.000$; right: $\phi_{iso} = 1.000$. Example corner positions r are labeled, with the suffix d indicating the position in the dry stage and s indicating the position in the swollen state. The distances between r_1 and r_2 and r_1 and r_n are shown with a dashed line. All corner positions are marked with red circles in the dry state and blue circles in the swollen state.

S7 Shape dependence on y -direction

The deflection patterns of the membrane in binary isopropanol-water mixtures are described by equation 1. For all deflection patterns, $m = 1$ was observed. The deflection pattern seems to change continuously from $w = 0$ (figure S7a) with $\sin(\pi m y/b)$ (figure S7b) and finds its maximum at $y = 1/2 b$ (figure S7c).

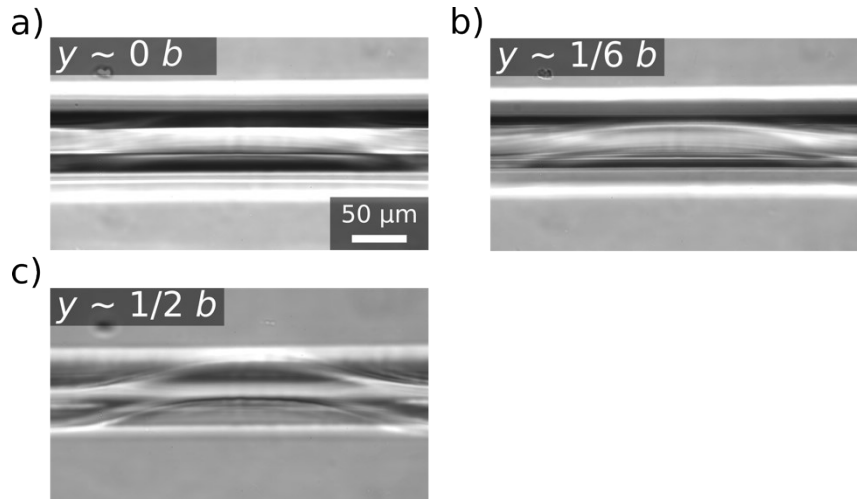
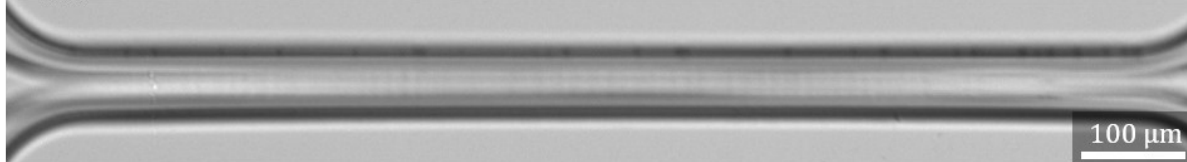


Figure S7: Micrograph of a single buckle form a deflection pattern at $\phi_{iso} = 1.000$. The micrographs were taken at different y -positions while holding x and z constant. a): $y \approx b$, b): $y \approx 1/6 b$, c): $y \approx 1/2 b$.

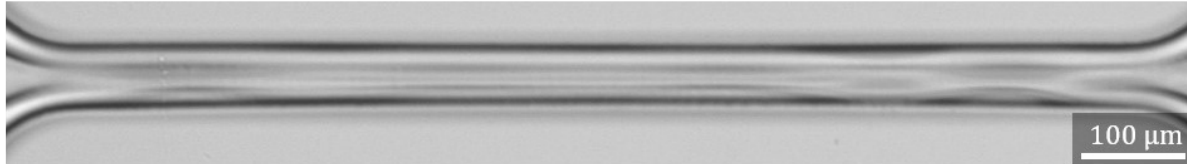
S8 Shape of the membrane at the buckling transition point

Micrographs with the shapes of the membrane for ϕ_{iso} around ϕ_b are shown in figure S8. For $\phi_{iso} = 0.960$ ($\phi_{iso} < \phi_b$) the membrane is straight and shows no out-of-plane deflections (figure S8a). At $\phi_{iso} = 0.968$ ($\phi_{iso} \approx \phi_b$), the membrane shows weak out-of-plane deflections, but no periodic buckling pattern is observed (figure S8b). At $\phi_{iso} = 0.972$ ($\phi_{iso} > \phi_b$), a periodic buckling pattern can be observed, which has characteristic $1/2\lambda$, w_{max} , n , and m values (figure S8c).

a) $\phi_{iso} = 0.960$



b) $\phi_{iso} = 0.968$



c) $\phi_{iso} = 0.972$

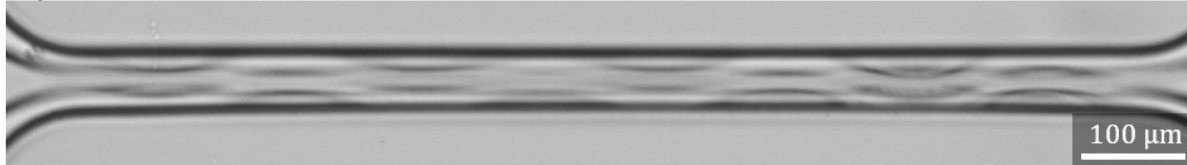


Figure S8: Membranes at ϕ_{iso} around ϕ_b : a) $\phi_{iso} = 0.960$ ($\phi_{iso} < \phi_b$), the membrane is straight and show no significant displacement form its initial position. b) $\phi_{iso} = 0.968$ ($\phi_{iso} \approx \phi_b$), the membrane shows small displacements form its initial position, but no regular buckling pattern with a well defined $1/2\lambda$. c) $\phi_{iso} = 0.972$ ($\phi_{iso} > \phi_b$), the membrane buckles in a well-defined buckling pattern.

S9 50 μm membrane

Two channels of $h_c = 50 \mu\text{m}$ with an embedded membrane of $h_m = 50 \mu\text{m}$, $b = 200 \mu\text{m}$, and $a = 1000 \mu\text{m}$ immersed in an isopropanol-water mixture of $\phi_{iso} = 1.000$ are shown in figure S9a. The membrane is straight and shows no out-of-plane deflections, while a membrane with $h_m = 20 \mu\text{m}$ and same a and b shows a buckling pattern. From equation 3 (main text) it can be seen that the buckling stress depends on the inverse aspect ratio $\sigma_b \propto (h_m/b)^2$. By increasing h_m by a factor of 2.5, σ_b rises above a level, which cannot be reached by swelling with isopropanol water mixtures. By comparing $R^*(\phi_{iso})/\eta$ of the devices of different h_m/b for ϕ_{iso} between 0.000 and 1.000, in the experiments using a $h_m = 50 \mu\text{m}$ device no change in $R^*(\phi_{iso})/\eta$ (almost constant regardless of ϕ_{iso}) can be observed, while in the $h_m = 20 \mu\text{m}$ devices a rapid increase of $R^*(\phi_{iso})/\eta$ for $\phi_{iso} > \phi_b$ (figure S9b) is observed.

$\phi_{iso} = 1.000, b/h_m = 4$

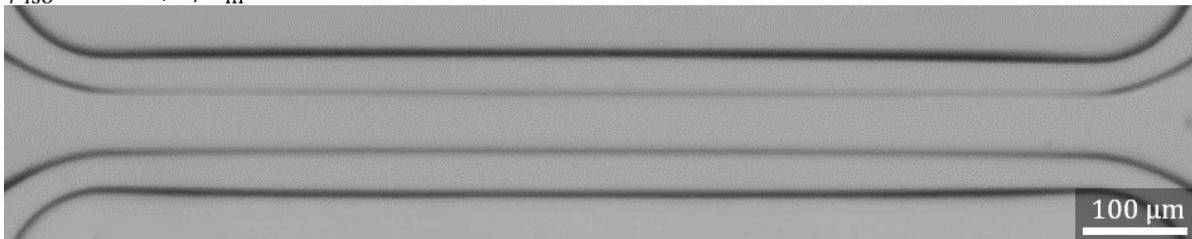


Figure S9a: Membrane with $b/h_m = 4$, in isopropanol-water mixture of $\phi_{iso} = 1.000$.

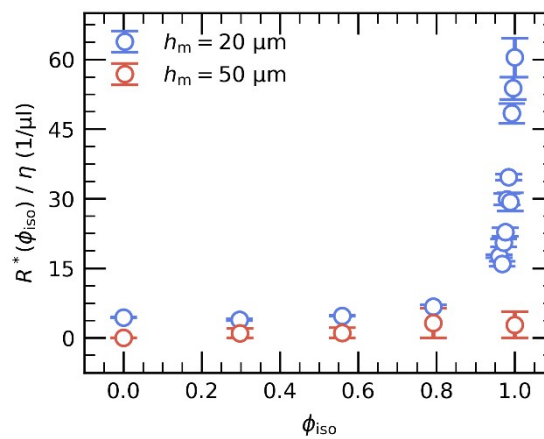


Figure S9b: $R^*(\phi_{iso})/\eta$ of isopropanol-water mixtures flowing through microfluidic devices with membranes of different h_m . Blue: $h_m = 20 \mu\text{m}$ with a buckling point at $\phi_b = 0.968$. Red: $h_m = 50 \mu\text{m}$, which does not show a buckling point for binary isopropanol-water mixtures.

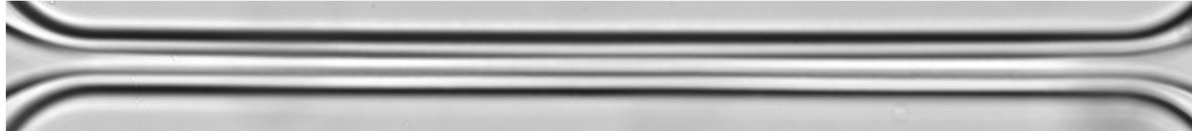
S10 Swelling of membranes in isopropanol-ethanol mixtures

The membrane shows different behavior when exposed to isopropanol-ethanol mixtures in comparison to isopropanol-water mixtures (figure S10). In isopropanol-ethanol mixtures no out of plane deflections are observed for ϕ_{iso} between 0.000 and 0.449 (figure S10a & b). The membrane starts deflecting out of plane at $\phi_{iso} = 0.499$ (figure S10c) and a regular buckling pattern is observed from $\phi_{iso} = 0.649$ (figure S10d), from which n decreases and r_{max} increases in a similar way as for isopropanol-water mixtures (figure S10d & e). At $\phi_{iso} = 1.000$ the membrane reaches the same buckling pattern (figure S10e).

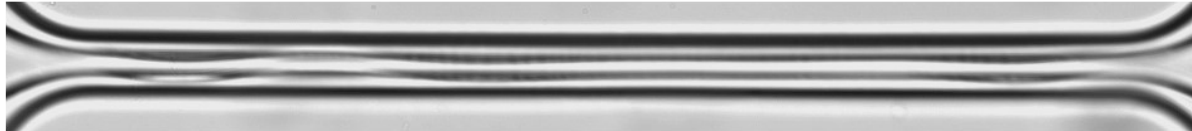
a) $\phi_{iso} = 0.000, \phi_{EtOH} = 1.000$



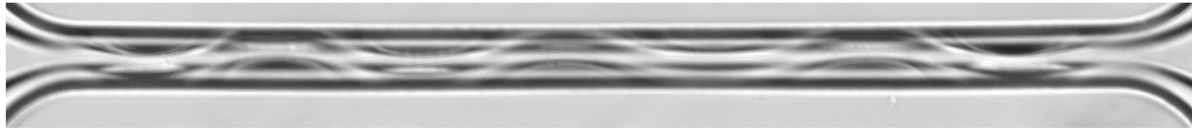
b) $\phi_{iso} = 0.449, \phi_{EtOH} = 0.551$



c) $\phi_{iso} = 0.499, \phi_{EtOH} = 0.501$



d) $\phi_{iso} = 0.649, \phi_{EtOH} = 0.351$



e) $\phi_{iso} = 1.000, \phi_{EtOH} = 0.000$

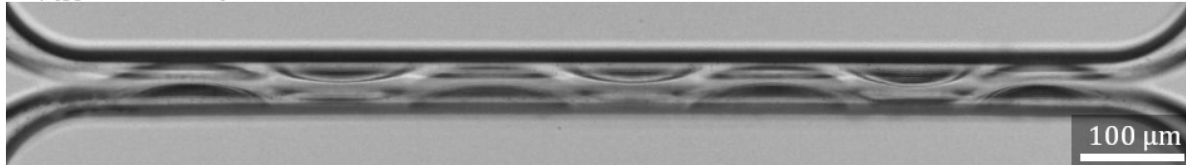


Figure S10: Deflection of the membrane exposed to isopropanol-ethanol mixtures of different isopropanol volume fractions ϕ_{iso} and ethanol volume fractions of $\phi_{EtOH} = 1 - \phi_{iso}$.

S11 Shape of buckling membranes under flow conditions/applied pressure difference

By applying Δp between the inlet and the outlet of the microfluidic device a pressure-driven viscous flow through the microfluidic channels passing the membrane was induced. The pressure difference was small enough not to perturb the shape of the membrane. Exemplarily the micrograph of the membrane at $\phi_{iso} = 0.976$ exposed at different Δp are shown in figure S11a) with $\Delta p = 4.2 \text{ hPa}$ and b) with $\Delta p = 32.2 \text{ hPa}$. The deflection pattern maintains its shape for the measured Δp (λ , w_{max} , n , and m remain constant).

a) $\phi_{iso} = 0.976, \Delta p = 4.2 \text{ hPa}$



b) $\phi_{iso} = 0.976, \Delta p = 32.2 \text{ hPa}$

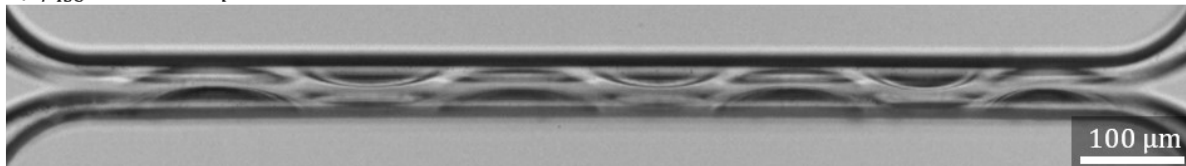


Figure S11: Micrograph of buckling membrane exposed to an isopropanol-water mixture with $\phi_{iso} = 0.976$. The pressure-driven flows of isopropanol-water mixtures were caused by different Δp : a) 4.2 hPa b) 32.2 hPa .

References

- ¹ T. Tanaka, *Stat. Mech. Appl.*, 1986, **140A**, 261-268.
- ² T. Tanaka, D. J. Fillmore, *J. Chem. Phys.*, 1979, **70**, 1214-1218.